

Precision searches in dijets at the HL-LHC and HE-LHC

S. V. Chekanov, J. T. Childers, J. Proudfoot, R. Wang

*HEP Division, Argonne National Laboratory,
9700 S. Cass Avenue, Argonne, IL 60439, USA*

D. Frizzell*

*Homer L. Dodge, Department of Physics and Astronomy,
University of Oklahoma, Norman, OK, USA*

(Dated: April 2, 2018)

Abstract

This paper explores the physics reach of the High-Luminosity Large Hadron Collider (HL-LHC) for searches of new particles decaying to two jets. We discuss inclusive searches in dijets and b -jets, as well as searches in semi-inclusive events by requiring an additional lepton that increases sensitivity to different aspects of the underlying processes. We discuss the expected exclusion limits for generic models predicting new massive particles that result in resonant structures in the dijet mass. Prospects of the Higher-Energy LHC (HE-LHC) collider are also discussed. The study is based on the Pythia8 Monte Carlo generator using representative event statistics for the HL-LHC and HE-LHC running conditions. The event samples were created using supercomputers at NERSC.

PACS numbers: 12.38.Qk, 13.85.-t, 14.80.Rt

* Also affiliated with the HEP Division, Argonne National Laboratory, 9700 S. Cass Avenue, Argonne, IL 60439, USA

I. INTRODUCTION

Heavy particles decaying to two jets are a generic consequence of many Beyond-the-Standard Model (BSM) theories. Recently, searches in dijet mass distributions at the LHC have been performed by both ATLAS and CMS collaborations [1–6] using run I and run II LHC data. An extension of such studies at the High-Luminosity LHC (HL-LHC) and the Higher-Energy LHC (HE-LHC) colliders will be an important goal of the energy frontier.

In the past, searches in dijets at the LHC were mainly focused on the high-mass tail of dijet distributions, rather than on the bulk of data (below 1 TeV). This is related to the fact that the collection of inclusive dijet events with dijet masses of the order of hundreds of GeV is reduced (or “pre-scaled”) at the trigger level in order to cope with a large rate of multijet QCD events. Focusing on the tail of dijet-mass distributions (M_{jj}), rather than on the data in the region close to the electroweak (EWK) scale, < 1 TeV, limits the potential of searches in inclusive dijet masses below 1 TeV.

Requiring a lepton, photon and or other identified objects with relatively low transverse momentum ($p_T < 0.1$ TeV), allows searches for new particles through associated production in dijet masses using the main fraction of collected data. This can lead to detailed studies of dijets at relatively low masses ($0.1 < M_{jj} < 1$ TeV), while reducing contributions from QCD multijet events, which represent the main background for inclusive dijet mass searches. The multijet QCD background can further be reduced for dijets where one or two jets are tagged as b -jet. High-precision searches focusing on the medium range of invariant masses in semi-inclusive final states was discussed in [7] in the context of a broad class of Hidden Valleys models [8], in which new particles can be as light as the Standard Model (SM) particles, i.e. with masses below 1 TeV.

The studies of dijets involve many technical challenges for future experiments. The HL-LHC will deliver about 3 ab^{-1} of integrated luminosity, more than a factor 10 of the data that will be collected by the end of the LHC project. This amount of data opens a new chapter in BSM searches focusing on extraction of features in M_{jj} distributions where the relative statistical uncertainty (i.e. statistical uncertainty expressed as a fraction of data point value) can be as small as $10^{-4} - 10^{-3}$ near $M_{jj} = 0.1$ TeV as shown in this paper. As a first step to such studies, we will use Monte Carlo (MC) event generation with a representative event statistics to explore sensitivity to new states decaying to two jets, without simulations of

detector effects and pile-up contributions.

The goal of this paper is to understand the physics potential of the proposed HL-LHC and HE-LHC experiments with respect to searches for new states decaying to dijets for inclusive and semi-inclusive event selections, as well as to explore different methods designed for gaining more sensitivity to new physics. In the searched mass region from ~ 0.1 to 10 (20) TeV at the HL-LHC (HE-LHC), event rates fall by more than 14 orders of magnitude. Modeling mis-identification rates of leptons and b -jets in this large range of invariant masses is challenging since it requires certain experiment-motivated assumptions that can numerically be implemented in MC simulations, as well as an analysis of large event samples from MC generators that include parton showers and hadronization. We will discuss this topic using realistic MC event samples, creation of which has become possible with the use of high-performance computing. In addition, we will calculate the exclusion limits for BSM models predicting heavy particles decaying to two jets at the HL-LHC and HE-LHC. The limits will be calculated using MC simulations of inclusive dijets, b -jets and dijets associated with a lepton.

II. MONTE CARLO EVENT SIMULATIONS

The analysis presented in this paper was performed using the PYTHIA8 [9] MC generator with the default parameter settings and the ATLAS A14 tune [10] for minimum-bias events. The center-of-mass collision energy of pp collisions was set to 14 TeV and 27 TeV for the HL-LHC and HE-LHC respectively. The NNPDF 2.3 LO [11] parton density function, interfaced with PYTHIA8 via the LHAPDF library [12], was used. A minimum value of transverse momentum for the matrix elements for $2 \rightarrow 2$ processes was 40 GeV. The simulations were created for three categories of SM processes implemented in leading-order (LO) matrix elements, with the parton shower (PS) followed by hadronization:

- Light-flavor QCD dijets. This category of events includes ten $2 \rightarrow 2$ quark and gluon processes, including b -quark pair production, but excluding $t\bar{t}$ production from hard interactions, which is considered as separate below. We apply a phase-space re-weighting to increase the statistics in the tail of the M_{jj} distribution as discussed in [9].
- Vector and scalar boson production that includes the W Z , H^0 -boson processes avail-

able in PYTHIA8. This category of events has 23 processes at the $2 \rightarrow 1$ and $2 \rightarrow 2$ level. Due to the presence of the $2 \rightarrow 1$ processes, no phase space re-weighting was used.

- $t\bar{t}$ and single top quark production which includes six $2 \rightarrow 2$ processes. No phase-space re-weighting was applied.

Currently, we do not use simulations at next-to-leading-order (NLO) accuracy, or at tree-level LO matrix elements included in ALPGEN [13] or BLACKHAT [14], which typically lead to larger cross sections. Even with the use of supercomputers, the large data samples required for the statistical precision of this study preclude using these more computationally intensive programs.

The simulation tools, small portions of event samples and PYTHIA8 settings used in this study are available from the HepSim public event repository [15]. The studies presented in this paper, however, require significant statistics, thus keeping events on a disk is impractical. A faster and less storage-demanding solution based on generating parton-level events does not provide the required information, since the studies presented in this paper are based on distributions sensitive to mis-identification of light jets as leptons or b -jets. An analysis of large event samples from the complete simulation of the parton shower followed by hadronization is essential. A simple scaling of low-statistics distributions to a luminosity of the order of several ab^{-1} leads to significant fluctuations in M_{jj} bins, even after the phase space re-weighting used in this paper.

In view of the above difficulties, we chose to perform the generation and analysis in series on a supercomputer. To achieve this, a Docker/Singularity container image of the HepSim software was created and deployed on the Cori supercomputer (Phase 2, Intel Knights Landing cores) of the National Energy Research Scientific Computing Center (NERSC). The software image includes the PYTHIA8 MC generator and the complete HepSim software stack for jet reconstruction and the final analysis. The maximum value of the PYTHIA8 seed ($9 \cdot 10^8$) is not very high for massively parallel jobs, therefore, special care was taken to avoid creation of duplicate events. The calculations took about 10 million core-hours over a ten day period. The analysis used about 100 billion MC events for the three process categories discussed above at the centre-of-mass energies of 14 TeV and 27 TeV.

The simulated number of background events for $M_{jj} < 1$ TeV is several orders of mag-

nitude smaller than what is needed for the analysis of M_{jj} distributions from the HL-LHC. For example, the cross section for multijet events with the 40 GeV cut on the LO matrix elements for $2 \rightarrow 2$ processes in pp collisions at 14 TeV is $7.3 \cdot 10^{10}$ fb. The problem of low statistics is partially mitigated using the adopted phase-space re-weighting technique discussed above. As for any counting experiment the statistical uncertainty for each M_{jj} bin was defined as the square root of the bin height.

For the simulation of the signal events, we use a model with an extra gauge boson, Z' , that arises in many extensions [16] of the electroweak symmetry of the Standard Model. The signal events were generated using the PYTHIA8 generator with the default settings, ignoring interference with SM processes, with a width of about 15% of the Z' mass. This width is usually considered as the maximum width of a resonance in ATLAS searches [1, 3]. We consider two cases for Z' decays, one in which Z' decays to light-flavor quarks, and one with only b -quark decays.

As discussed in the introduction, pile-up events were not included in the simulation. Mixing billions of generated events with 140-200 low- p_T “minimum bias” events is beyond the technical capability of the computational resources used for this work. We should note, however, that pile-up events are not expected to change our conclusions related to high- p_T physics above the TeV scale. In addition, the LHC experiments have developed successful techniques to mitigate pile-up effects. Such techniques should be considered in conjunction with detector-level objects (such as calorimeter clusters, or tracks associated with the primary interaction vertex), all of which are beyond the scope of this paper.

III. EVENT RECONSTRUCTION

Hadronic jets were reconstructed from stable particles, which are defined as having a lifetime more than $3 \cdot 10^{-10}$ seconds. Neutrinos were excluded from consideration. The jets were reconstructed using the anti- k_T algorithm [17] as implemented in the FASTJET package [18]. The jet algorithm used a distance parameter of $R = 0.4$. The minimum transverse momenta of jets was 40 GeV, and the pseudorapidity of jets was $|\eta| < 2.4$.

The minimum transverse momentum of the leptons used in this analysis was set to 60 GeV. To reduce the mis-identification rates, the leptons are required to be isolated. A cone of the size 0.2 in the azimuthal angle and pseudo-rapidity is defined around the true

direction of the lepton. Then, all energies of particles inside this cone are summed. A lepton is considered to be isolated if it carries more than 90% of the cone energy.

As full simulation is not within the scope of this study, we estimate the rate of misidentification of muons (the muon fake rate) as a fraction, 0.1%, of the jet rate similar to the ATLAS study [19]. This is implemented by assigning the probability of 10^{-3} for a jet to be identified as a muon using a random number generator. We do not use electrons since their fake rate is a factor of ten larger than for muons.

Dijet invariant masses, M_{jj} , were reconstructed by combining the two leading jets having the highest $p_T(jet)$. The minimum value of M_{jj} was chosen to be 125 GeV, which is large enough to avoid biases arising from the jet selection and contributions from the W/Z decays. At the same time, this value well represents the bulk of the anticipated HL-LHC data where the M_{jj} distribution smoothly decreases with increase of M_{jj} . This feature is important for our discussion in Sect. VII.

A reproduction of the experimental mis-tag rate of b -jets is difficult for the generator-level MC studies. Generally, the mis-tag rate depends on many factors, including a dependence on $p_T(jet)$ [20]. For the studies involving b -jets, we assume a constant 10% mis-tag rate. This value is sufficiently realistic [20] for large $p_T(jet)$ considered in this paper and, at the same time, can easily be reproduced or modified in future studies. This mis-tag rate was implemented by using the probability of 0.1 for a light jet to be identified as a b -jet. The b -jets are additionally selected by requiring: (1) the ΔR between the b -quark and jet to be less than 0.4; (2) the b -quark p_T is at least 50% of the jet p_T .

This paper, being based on the generator-level Monte Carlo samples, does not include simulations of detector efficiencies for reconstruction of jets, leptons and b -tagging. The inclusion of efficiencies may change the exclusion limits shown in this paper, but they are unlikely to change comparisons between the HL-LHC and HE-LHC scenarios.

IV. DIJETS IN INCLUSIVE EVENTS

Figure 1 shows the M_{jj} distribution in PYTHIA8 for two different integrated luminosities, 100 fb^{-1} and 3 ab^{-1} . The bin size used in this figure gradually increases from 13 GeV for the lowest considered value of M_{jj} to 190 GeV near $M_{jj} = 10 \text{ TeV}$. Such variable-size bins were previously used in [1–3] in order to minimize jet resolution effects, and to reduce statistical

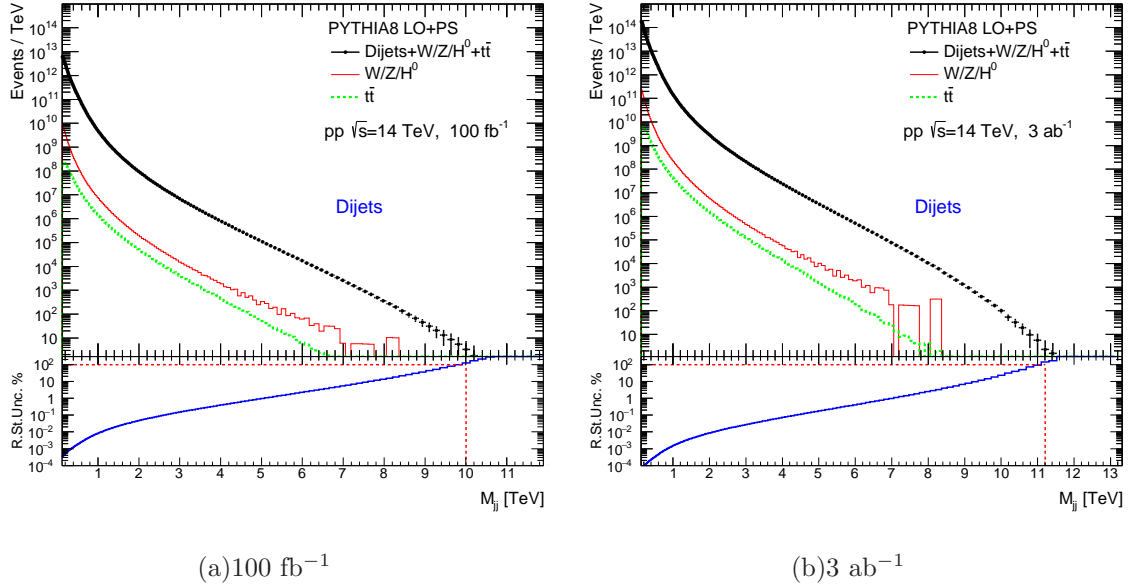


FIG. 1. Expectations for the dijet invariant mass distribution for 100 fb^{-1} (3 ab^{-1}) for the LHC (HL-LHC) using the PYTHIA8 generator. Contributions from $W/Z/H^0$ -boson processes and top-quark processes are shown separately (without stacking the histograms). The bottom plot shows the relative statistical uncertainty for each bin, together with the line indicating the mass point at which the uncertainty is 100%.

fluctuations in the tail of the M_{jj} distribution.

Figure 1 shows the sum of the three contributions discussed in Sect. II, together with the two contributions from $W/Z/H^0$ -boson processes combined and top-quark processes from the hard interactions (shown separately). The rate of the latter two processes combined near $M_{jj} = 0.5 \text{ TeV}$ is 0.1% of the total SM prediction. At the same time, the contribution from the $t\bar{t}$ production is only 0.02% of the total event rate. The lower panel shows the relative statistical uncertainty on the data points, i.e. $\Delta d_i/d_i$, where d_i is the number of the events in the bins, and Δd_i its statistical uncertainty (which is $\sqrt{d_i}$ in the case of counting statistics).

For a quantitative characterization of the dijet mass reach, we choose to define the M_{jj} point at which the relative statistical uncertainty in a bin is 100% (or $\Delta d_i/d_i = 1$), as indicated in the lower panel of Fig. 1 with the dash line. In the case of counting statistics, this corresponds to one entry per bin. In this study, the point at $\Delta d_i/d_i = 1$ is determined from many weighted events created by the PYTHIA8 event generator.

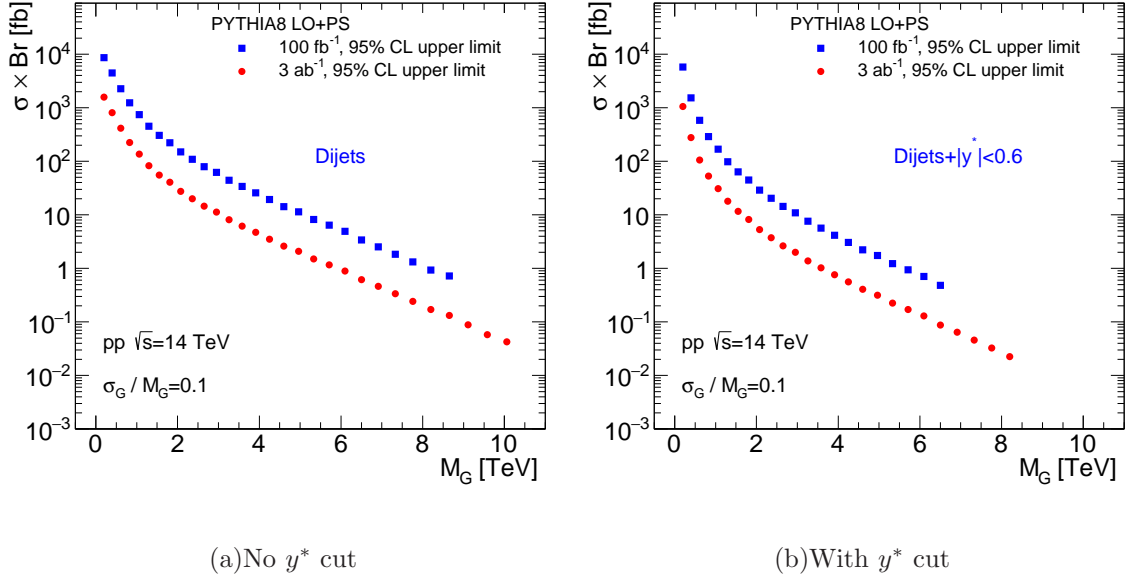


FIG. 2. The 95% C.L. upper limits obtained from the M_{jj} distribution on fiducial cross-section times the branching ratio to two jets for a hypothetical BSM signal approximated by a Gaussian contribution to the dijet mass spectrum. The limits are obtained (a) without and (b) with y^* cut.

Figure 2 shows the 95% credibility-level (C.L.) upper limit on fiducial cross-section times the branching ratio for a generic Gaussian signal with the width (σ_G) being 10% of the Gaussian peak position. The 95% quantile of the posterior is taken as the upper limit on the possible number of signal events in data corresponding to that mass point. This value, divided by the corresponding luminosity, provides the upper limit on the production cross section of a new particle times the branching ratio (Br) to two jets. In addition to the inclusive jet case, we also calculate the upper limits after applying the rapidity difference requirement $|y^*| < 0.6$ between two jets [21] in order to enhance the sensitivity to heavy BSM particles decaying to jets.

In order to calculate the expected upper limits for realistic shapes of the dijet mass distribution from heavy exotic particles, such as Z' , we have performed a simulation of Z' decays to jets, assuming the width of 15% of the Z' mass. The comparison of the Gaussian shape with the signal shape from the Z' decays in PYTHIA8 is shown in Fig. 3. The generated masses of the Z' particles are given by the Breit-Wigner distribution, but the M_{jj} distributions are asymmetric, which are typical for reconstructed dijet masses using realistic jet algorithms (note the logarithmic scale used for this figure).

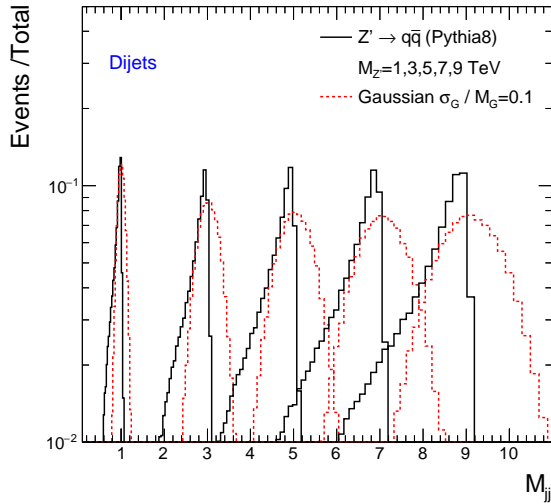


FIG. 3. The shapes of the M_{jj} distributions for a hypothetical BSM signal approximated by a Gaussian contribution (red dash lines) and for the $Z' \rightarrow jets$ used for the calculation of the 95% C.L. upper limits (black solid line).

Alternatively, exclusion limits were calculated using the CL_s method with a binned profile likelihood ratio as the test statistic using the HISTFITTER framework [22]. The expected limits on the signal model are calculated by using an asymptotic approximation [23]. Figure 4 shows the 95% C.L. upper limits. The green and yellow bands represent the 1σ and 2σ probability intervals around the expected limit. The obtained limits are found to be rather similar to the Gaussian limits (without the requirement $|y^*| < 0.6$) obtained above, despite the difference in the signal shape. Unlike the Gaussian limits, the HISTFITTER limits were calculated starting from $M_{jj} > 1$ TeV. Below this value, the HISTFITTER technique produces an unstable result caused by fluctuations in the M_{jj} distribution after the extrapolation of the low-statistics histogram to the required luminosity (see Sect. II).

The limits shown in Fig. 4 can be used for exclusion of models predicting peaks in the M_{jj} distributions. Several BSM benchmark models, such as models of quantum black holes, excited quarks, W' and Z' , have been excluded by CMS and ATLAS using LHC run I and run II data [1–6]. Therefore, we do not show the cross sections for such BSM models in Fig. 2 and 4.

The PYTHIA8 expectations for the M_{jj} distribution for the HE-LHC are shown in Fig. 5. The dijet mass distribution uses bin sizes that gradually increase from 13 GeV for the lowest

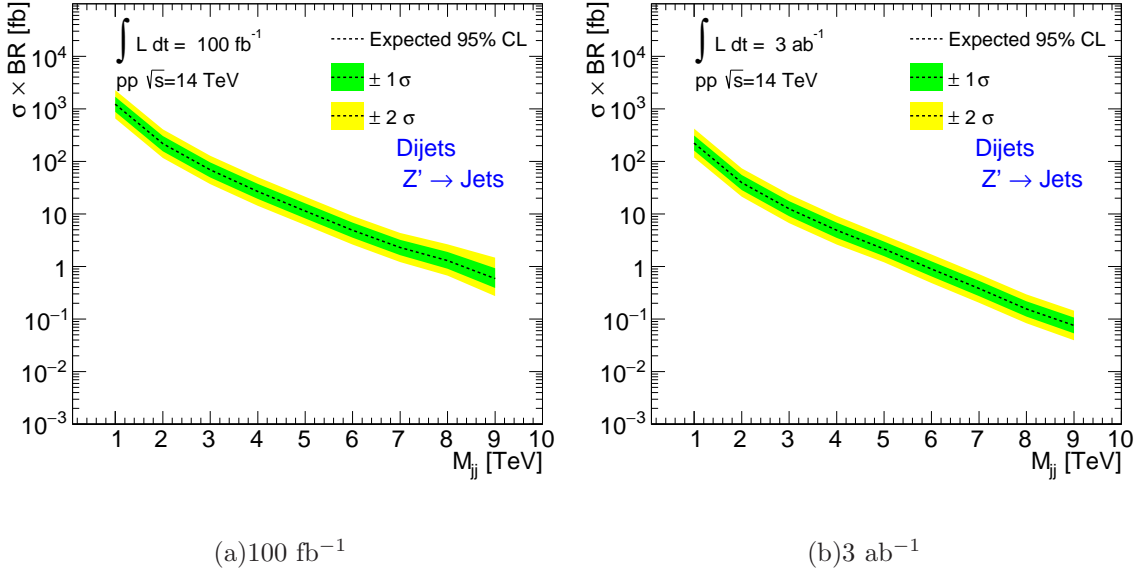


FIG. 4. The 95% C.L. upper limits obtained from the M_{jj} distribution on cross section times the branching ratio to two jets for a Z' particle decaying to two jets.

value of M_{jj} to 280 GeV near $M_{jj} = 10$ TeV. The lower panel shows the relative statistical uncertainties together with the line indicating the mass at which the relative statistical uncertainty on the data point is 100%. Figure 6 shows the mass reach as a function of integrated luminosity for the HL-LHC and HE-LHC, defined by the point at which the relative statistical uncertainty is 100%. The M_{jj} mass reach at the centre-of-mass of 27 TeV is close to 17 TeV, even for the modest luminosity of 100 fb^{-1} . This is a factor of two larger than the dijet mass reach for the luminosity expected at the HL-LHC.

Figure 7 shows the 95% C.L. upper limits on the product of the cross section and the branching ratio for a signal approximated by a Gaussian whose width is 10% of the mass of the searched resonance. The expected limit for 3 ab^{-1} is a factor of ten better than for 100 fb^{-1} .

V. DIJETS IN EVENTS WITH ASSOCIATED MUONS

The previous studies of inclusive dijets represent a hypothetical scenario that may never be realized in practice due to difficulties [24] in analyzing data with trigger prescales applied to jets at medium p_T . However, measurements of unbiased M_{jj} distributions (below 1 TeV)

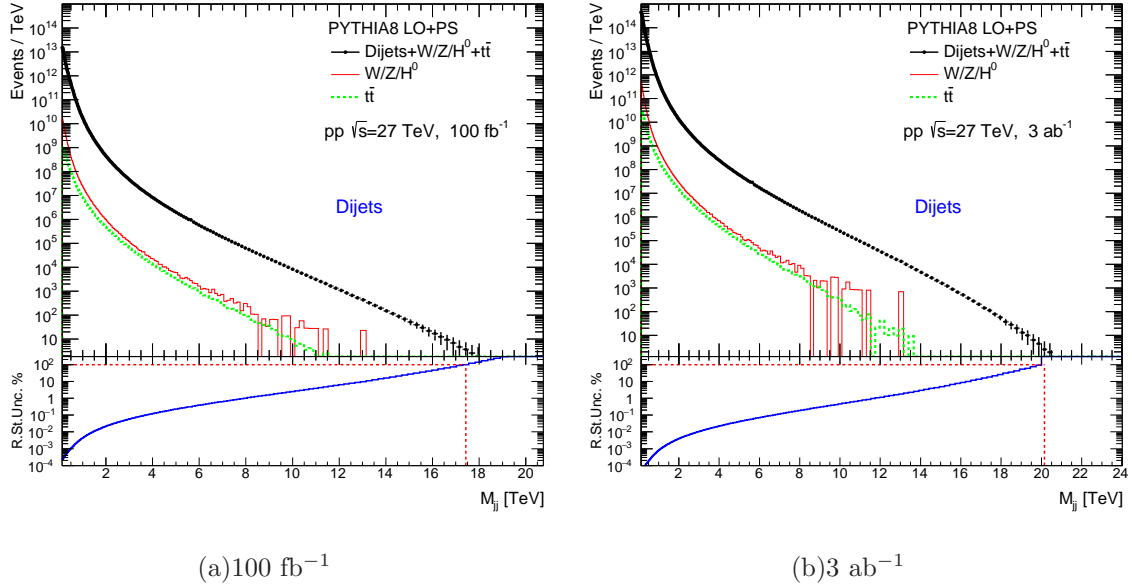


FIG. 5. The distribution of the dijet invariant masses for 100 fb^{-1} and 3 ab^{-1} at the HE-LHC, together with the relative statistical uncertainty shown in bottom panel.

can be made possible by using an independent object to trigger on. For example, to reduce the impact of the very high rate of multi-jet background, at the price of requiring associated production, one can require an isolated muon, electron or other particle.

Figure 8(a) shows the dijet invariant masses with associated leptons with $p_T(l) > 60 \text{ GeV}$ using the isolation requirements as described in Sect. III. This figure corresponds to the ideal case when the lepton mis-identification rate is set to zero. The fraction of the combined $W/Z/H^0$ and top events to the total predicted event rate is 96%. This shows that any new physics that leads to resonances with the production rates compatible with $W/Z/H^0$ processes can easily be detected, unlike the case with fully inclusive jets discussed in the previous section.

To illustrate a scenario with lepton mis-identifications, let us now turn to the case with muons. Figure 8(b) shows the M_{jj} distribution with isolated muons, including contributions from jets which are mis-identified as muons. The mis-identification rate is set to 0.1% as discussed in Sect. III. According to Fig. 8(b), the fraction of $W/Z/H^0$ /top processes is 1.2% to the total event rate, which is a factor of ten larger than for the inclusive dijets shown in Fig. 1. Figure 8(a) and (b) shows that the contribution from EWK and top processes to the total event rate strongly depends on the mis-identification rates for leptons. For

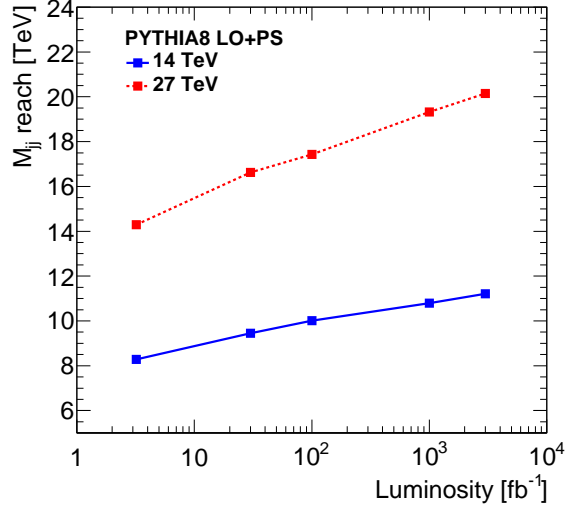


FIG. 6. Dijet mass reach for the HL-LHC and HE-LHC experiments. The uncertainties on the data points, derived from the bin width used for the simulated M_{jj} distributions, are compatible with the size of the symbols.

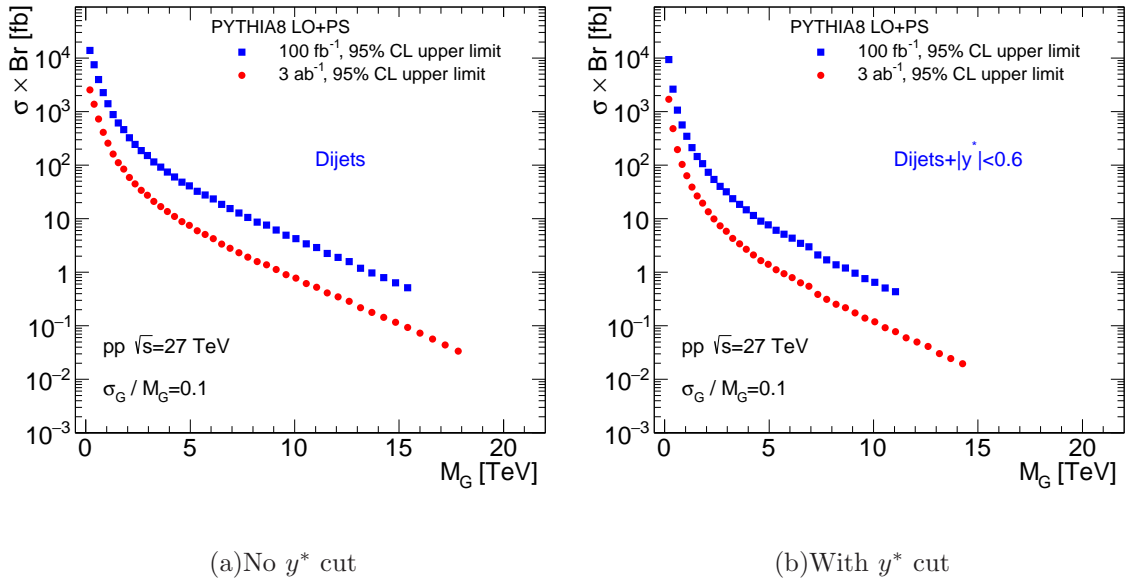


FIG. 7. The 95% C.L. upper limits obtained from the M_{jj} distribution on the cross section times the branching ratio to two jets for a hypothetical signal approximated by a Gaussian contribution to the expected dijet mass. The HE-LHC expectations were obtained using the PYTHIA8 generator.

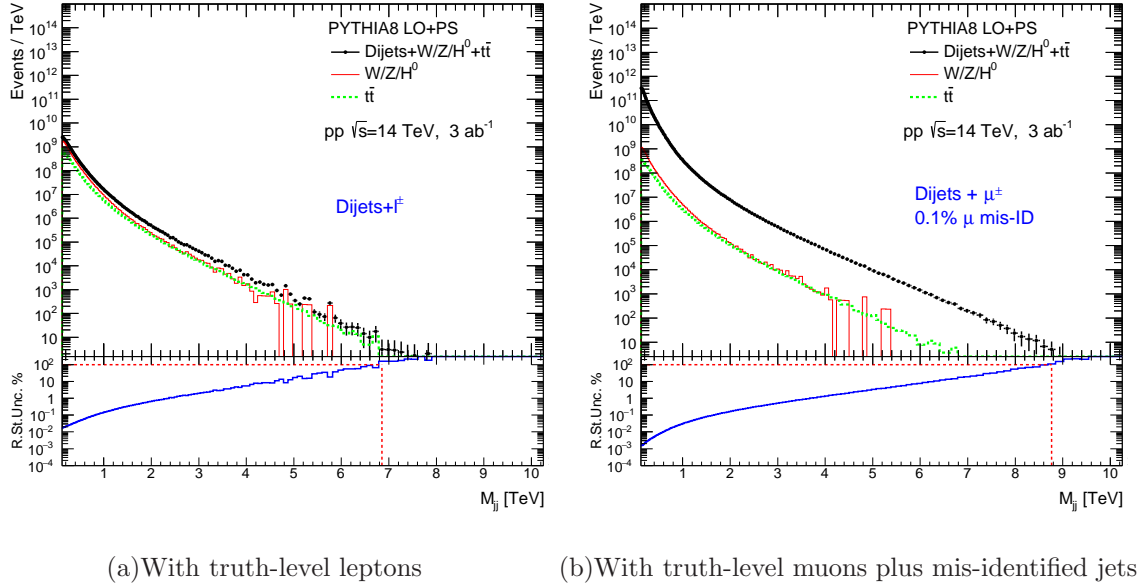


FIG. 8. Dijet invariant masses with associated leptons for 3 ab^{-1} of the HL-LHC experiment. The distributions are shown for (a) dijets with muons and electrons without mis-identification and (b) for muons assuming 0.1% mis-identification rate.

realistic scenarios, exact fractions of EWK and top contributions should be calculated using full detector simulations.

As for the previous sections, our goal is to give expectations for exclusion limits at the HL-LHC and HE-LHC using assumed muon fake rates, without discussing the cross sections for particular exotic models predicting enhancements in dijet masses. The 95% credibility-level upper limits for a signal for the muon-associated dijet production, assuming 0.1% mis-identification rate, are shown in Fig. 9. The signal was approximated by a Gaussian distribution whose width is 10% of the mass of the searched resonance. The figure shows the expectations for the HL-LHC and HE-LHC. Figure 10 shows the 95% credibility-level upper limits for a Z' signal comparing 100 fb^{-1} from the LHC with the HL-LHC luminosity scenario.

VI. STUDIES OF b -JETS AT THE HL-LHC AND HE-LHC

Now we consider the case with b -jets selected as described in Sec. III. Figure 11 shows the M_{jj} predictions for the sum of the three contributions (QCD dijets, vector/scalar boson

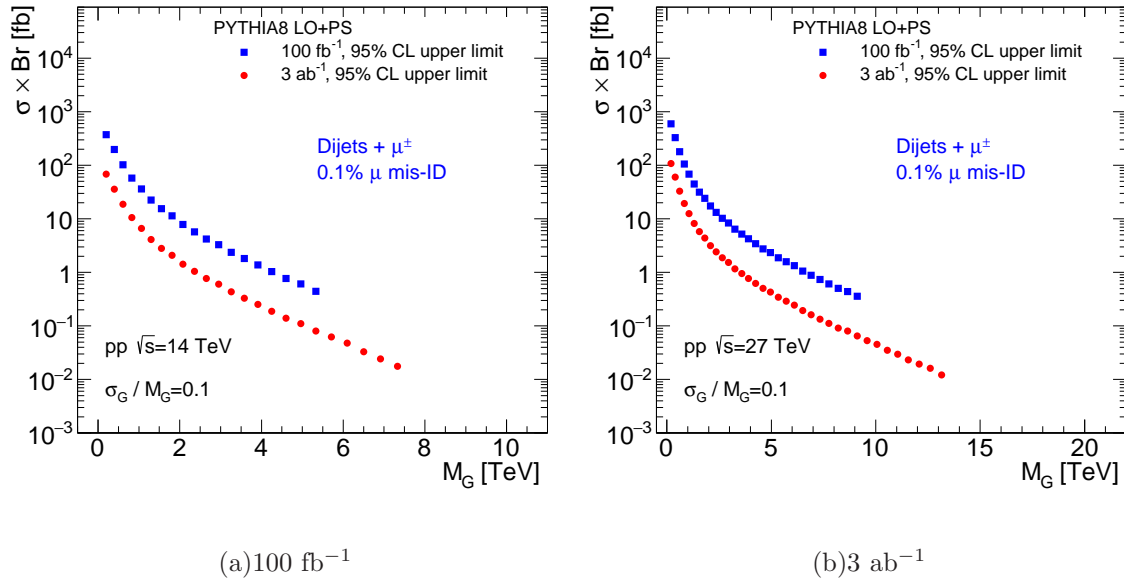


FIG. 9. The 95% C.L. upper limits obtained from the M_{jj} distribution on cross-section times the branching ratio to two jets with isolated muons for a hypothetical BSM signal approximated by a Gaussian contribution to the expected dijet mass. The limits were calculated for the HL-LHC and HE-LHC.

and top production) discussed in Sect. II, together with the two contributions from $W/Z/H^0$ -boson processes and top-quark processes from the hard interactions. The total event rate is about 2% of the inclusive dijet after b -tagging. The rate of the $W/Z/H^0$ and top processes combined near $M_{jj} = 0.5$ TeV is about 0.2% of the total event rate. The contribution from the $t\bar{t}$ production is larger than that from the $W/Z/H^0$ -boson processes.

Figure 12 shows the 95% C.L. upper limit for the cross section times the branching ratio for a signal approximated by a Gaussian whose width is 10% of the mass of the searched resonance. In addition to the dijet masses, we also calculate the upper limits after applying the rapidity difference requirement $|y^*| < 0.6$ between the two jets [2, 21].

In order to calculate the expected upper limits for observation of particles such as Z' , we have performed a simulation of Z' decays to b -jets, assuming that its width is 15%. Exclusion limits were also calculated using the CL_s method with a binned profile likelihood ratio as the test statistic using the HISTFITTER framework. Figure 12 shows the 95% C.L. upper for the realistic signal shapes.

Several BSM models, such as b^* and leptophobic Z' , predict peaks in the M_{jj} distribution,

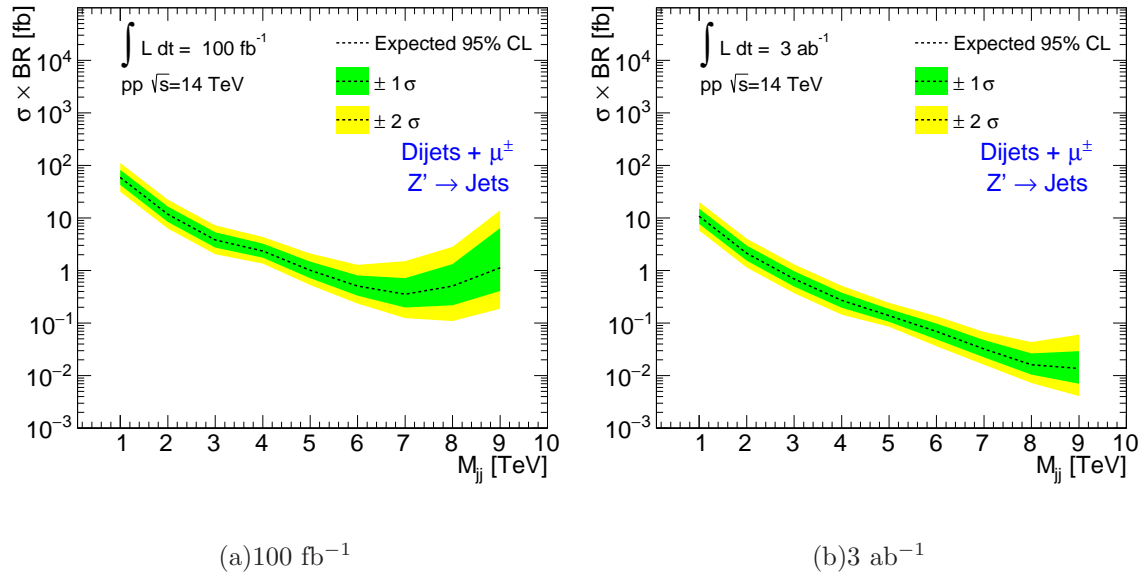


FIG. 10. The 95% C.L. upper limits obtained from the M_{jj} distribution on the cross-section times branching ratio for a hypothetical BSM process producing a resonance in the dijet mass distribution and is produced in association with an isolated muon, approximating the width of the dijet resonance by a Gaussian distribution.

where one or two jets are identified as b -jet. Some models have already been excluded by ATLAS [2].

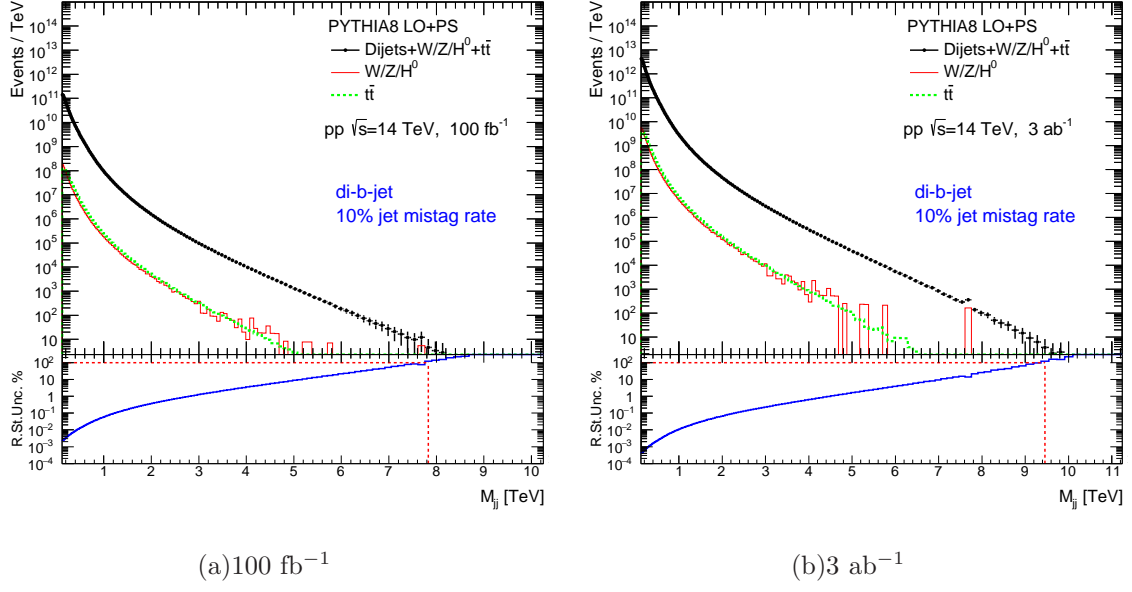


FIG. 11. The M_{jj} distributions for jets identified as b -jets, for 100 fb^{-1} and 3 ab^{-1} , together with the relative statistical uncertainty shown in bottom panel.

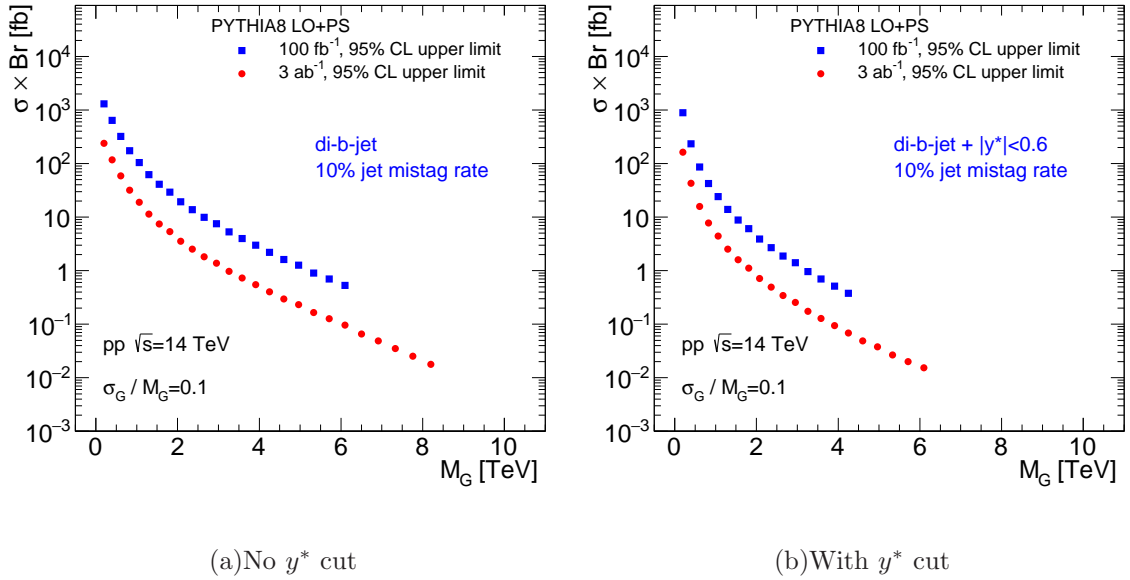
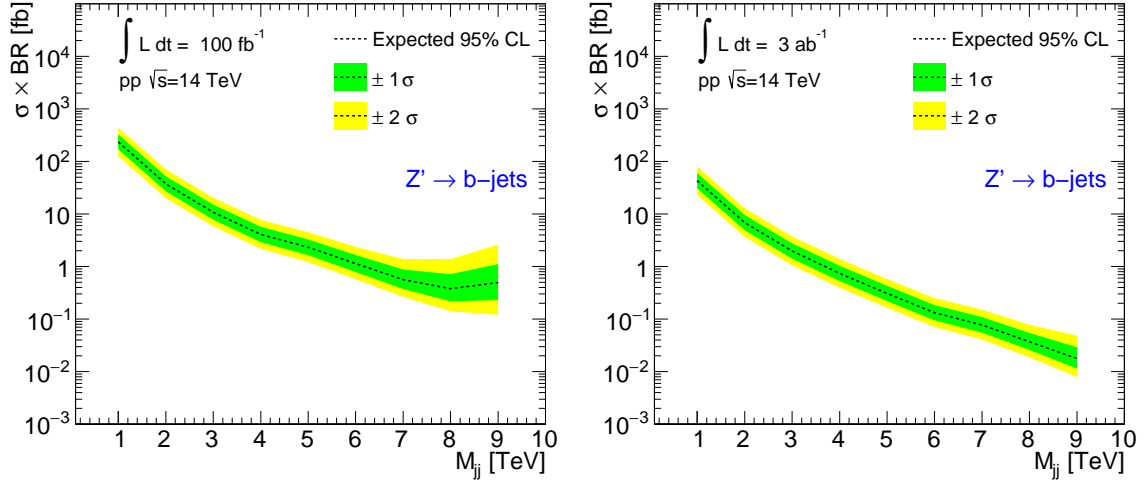


FIG. 12. The 95% C.L. upper limits obtained from the M_{jj} distribution on cross section times the branching ratio to two jets (identified as b -jets) for a hypothetical signal approximated by a Gaussian whose width is 10% of the mass of the searched resonance. The limits are shown (a) without and (b) with y^* cut.



(a) 100 fb^{-1}

(b) 3 ab^{-1}

FIG. 13. The 95% C.L. upper limits obtained from the M_{jj} distribution on cross section times the branching ratio to two jets for Z' particle decaying to two b -jets.

The PYTHIA8 expectations for the M_{jj} distribution with jets identified as b jets at the HE-LHC collider are shown in Fig. 14. The line on the lower panel indicates the mass at which the relative statistical uncertainty is 100% on the data point. As before, this point is chosen to define the dijet mass reach to be accessible for the given luminosity. This point may depend on the assumption used for the fake rate and the efficiency discussed in Sect. III, but the difference between different luminosity scenarios should not depend much on these assumptions. Figure 15 shows the mass reach for the HL-LHC and HE-LHC. For the modest luminosity of 100 fb^{-1} , the mass reach at the HE-LHC is above 13 TeV, which is a factor of two larger than for the HL-LHC, assuming that the reconstructed efficiencies and fake rates for b -jets are similar for the HE-LHC and HL-LHC.

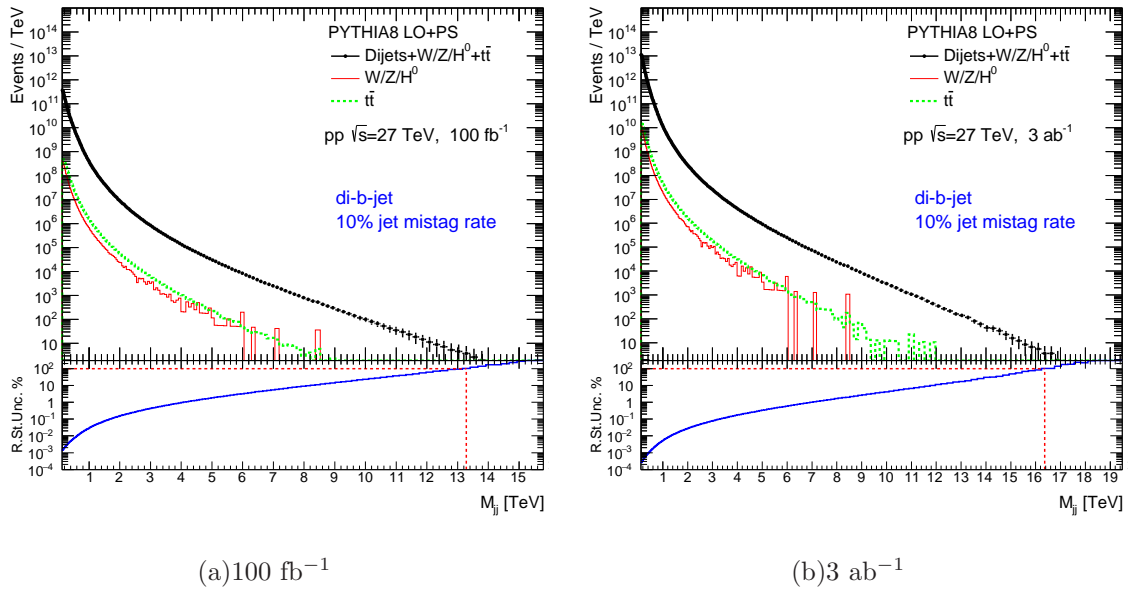


FIG. 14. Dijet mass distributions for jets identified as b -jets, for 100 fb^{-1} and 3 ab^{-1} at the HE-LHC.

Figure 16 shows 95% C.L. upper limits for the cross section times the branching ratio for a signal approximated by a Gaussian with $\sigma_G = 0.1 \cdot M_G$.

Now we will consider events with b -jets measured in events with an additional identified lepton. Figure 17(a)(b) shows the dijet invariant masses with isolated muons having $p_T > 60 \text{ GeV}$. The total event rate is reduced to 2% of the b -tagged dijet. It can also be noted that the contribution from $W/Z/H^0$ is at the level of 1.2% while the t -quark processes are at the level of 3%, which is a factor of ten larger than the contribution shown in Fig. 11 of

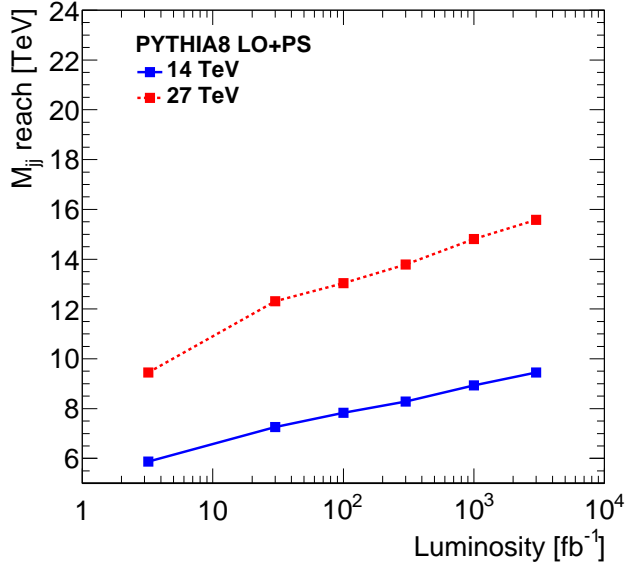


FIG. 15. Dijet mass reach for the HL-LHC and HE-LHC experiments for dijets identified as b -jets. The uncertainties on the data points, derived from the bin width used for the simulated M_{jj} distributions, are compatible with the size of the symbols.

Sect. VI.

For a completeness, Fig. 17(c)(d) show the 95% C.L. upper limits for the cross section times the branching ratio for a generic Gaussian signal, assuming the muon-associated dijet production. Figure 17(e)-(f) show the 95% C.L. upper limits for a $Z' \rightarrow b\bar{b}$ signal. Generally, the exclusion limits at a fixed mass obtained using 3 ab^{-1} are improved by a factor 10 compared to the 100 fb^{-1} case.

VII. SIGNAL EXTRACTION

The use of an associated lepton in the event selection allows a uniform exploration of the dijet mass distribution which spans 14 orders of magnitude in rate. The natural question arises how to extract features that may correspond to signal events from BSM physics. To illustrate the difficulties arising in a data-driven signal extraction, we will consider an analytic fit of dijet mass spectra with the monotonically decreasing function:

$$f(x) = p_1(1-x)^{p_2}x^{p_3+p_4 \ln x}, \quad (1)$$

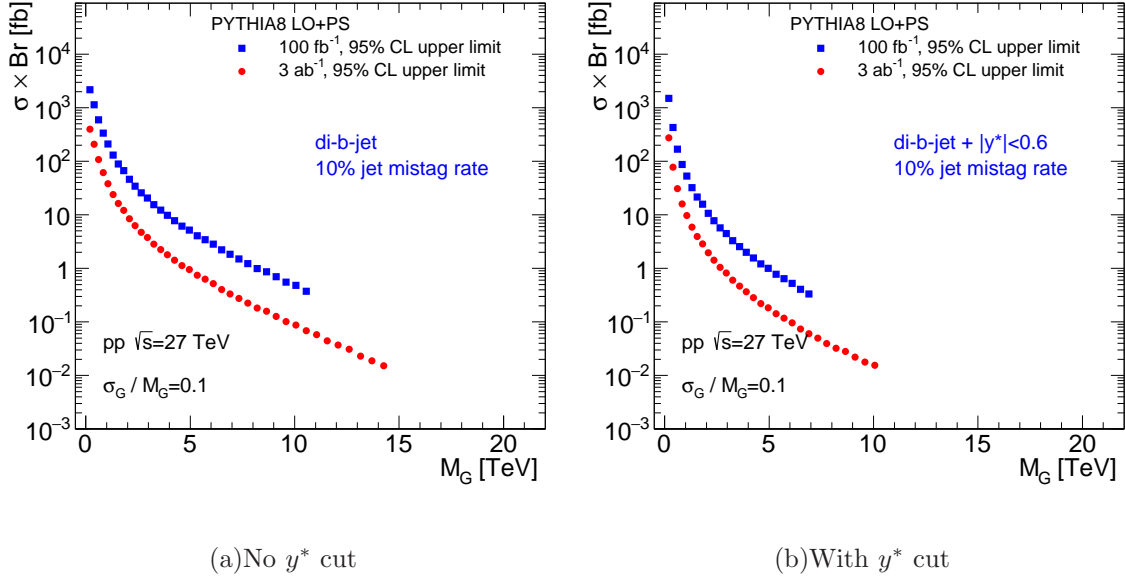


FIG. 16. The 95% C.L. upper limits obtained from the M_{jj} distribution on cross section times the branching ratio to two jets (identified as b -jets) for a hypothetical signal approximated by a Gaussian contribution to the expected dijet mass. The results are shown for the HE-LHC (without and with y^* cut).

were $x = M_{jj}/\sqrt{s}$ and p_i are fit parameters. This function was used for inclusive dijet searches [2, 3, 6] by both ATLAS and CMS collaborations.

Figure 18 shows the mass of two jets together with the fit of Eq. 1. The distribution for jets associated with isolated muons is shown in Fig. 18(b). The bottom plot shows the significance of deviations of the function from simulated data in terms of the variable $S_i = (d_i - f_i)/\Delta d_i$, where d_i is the simulated data point in a bin i , f_i is the value of the function after the χ^2 minimization, and Δd_i is the statistical uncertainty on the value of d_i . We consider the fit scenario when the function Eq. 1 is applied to the dijet mass spectrum below 1 TeV, and above 1 TeV, separately.

The fit function reasonably describes the mass distribution above 1 TeV. A similar good agreement between data and the fit function was shown in the previous studies [2, 3, 6] that used smaller integrated luminosities. When using the same integrated luminosity as in Ref. [2, 3, 6], no statistical deviations from the fit function were found. The quality of the fit was given by $\chi^2/ndf = 0.9$.

Figure 19 shows the mass of two jets associated with isolated muons together with the fit

of Eq. 1 for the HL-LHC case. In addition to the high-mass region, the figure shows the fit results for $0.125 < M_{jj} < 1$ TeV. This scenario is relevant for semi-inclusive searches using an additional trigger requirement on leptons, and other triggered particles. The function does describe the low-mass and high-mass regions in PYTHIA8, even when the fit was performed separately in these two mass windows. This can be seen from the quoted χ^2/ndf value, and by observing oscillations of S_i .

As a test, we have performed a χ^2 minimization with Eq. 1 using the M_{jj} distribution for inclusive dijets in different M_{jj} regions. To make sure that the observed feature does not come from the phase-space re-weighting (see Sect. II), the simulation was performed without the re-weighting, but using a smaller sample of events. Similar oscillating values of S_i were found. It was found that the fit cannot describe the entire mass spectra, $0.125 < M_{jj} < 1$ TeV, where it significantly underestimates the tail of the distribution. The fit also fails for the HE-LHC energies (not shown). A similar behavior in the fit was observed after multiplying the fit function by the additional term $x^{p_5 \ln^2 x}$.

Additional studies have been conducted by taking numerical derivatives of the function Eq. 1. It was found that the first derivatives of the function and data are monotonically increasing, while the second derivatives are always positive and do not cross the value zero. Therefore, the oscillatory behavior of S_i after the χ^2 minimization is a reflection of differences between the shape of the M_{jj} distribution in PYTHIA8 and the analytic function, rather than a consequence of the presence of oscillations in the simulated data.

Our results show that there are many challenges at the HL-LHC and HE-LHC in data driven methods to extract signals in the bulk of M_{jj} distribution, where the relative statistical uncertainties in M_{jj} bins reach 0.01%. The analytic approach based on Eq. 1 cannot describe the M_{jj} observed in PYTHIA8. Therefore, small features in the form of peaks from BSM physics can be masked by the oscillatory behavior of the fit residuals shown in Fig. 19. In addition to the fit function technique, numerical techniques for data-driven signal extraction may also be used, assuming they can reliably describe the shape for multijet QCD background and, at the same time, are sensitive to the presence of small peaks in dijet mass distributions. In the past, a number of peak-identification and data smoothing algorithms were proposed for counting-type observables [25]. An approach based on a sliding-window fitting technique was used by ATLAS [3] to overcome the complexity of M_{jj} distributions.

VIII. SUMMARY

This paper discusses the potential of precision searches in dijet invariant masses at the HL-LHC and HE-LHC. It was illustrated that the HE-LHC provides a significantly higher reach for dijet searches than the HL-LHC, even for rather modest 100 fb^{-1} luminosity. We provide the relevant 95% C.L. upper limits obtained from the M_{jj} distribution on cross-section times the branching ratio for BSM models predicting heavy particles decaying to two jets, including jets identified as b -jets. The limits at particle level were obtained for signals approximated with Gaussian distributions, as well as for Z' signal shapes created using PYTHIA8 MC.

The dijet masses in semi-inclusive events with associated leptons provides particularly interesting data for searches, since they can be well measured in a large range of dijet masses without biases from triggers, and are less affected by the large rate of inclusive jet events. We have illustrated that a data-driven determination of the shape background at the HL-LHC and HE-LHC should be performed with the relative statistical precision of 0.01% per data point for $M_{jj} < 1 \text{ TeV}$. It was shown that a requirement to observe an isolated muon increases sensitivity to vector-boson and top-quark production. With the expected statistical precision for the M_{jj} measurements, the HL-LHC and HE-LHC experiments will be sensitive to the shape of the M_{jj} distribution of these processes.

PYTHIA8 MC simulations were used for testing the data-driven approach used at the LHC for the extraction of BSM signals. When the fit function is applied to the M_{jj} distribution that matches the projected HL-LHC luminosity, we observe biases that limit detection of peaks in the M_{jj} distributions. Such biases are due to more complex shapes of the M_{jj} distributions in PYTHIA8, reflecting the underlying partonic kinematics, compared to the analytic function used at the LHC in the past.

ACKNOWLEDGMENTS

We thanks G. Bodwin, S. Mrenna and T. Sjöstrand for the discussion of the fit function used in this analysis. The submitted manuscript has been created by UChicago Argonne, LLC, Operator of Argonne National Laboratory (“Argonne”). Argonne, a U.S. Department of Energy Office of Science laboratory, is operated under Contract No. DE-AC02-

06CH11357. This research was made possible by an allocation of computing time through the ASCR Leadership Computing Challenge (ALCC) program. This research used resources of the National Energy Research Scientific Computing Center, a DOE Office of Science User Facility supported by the Office of Science of the U.S. Department of Energy under Contract No. DE-AC02-05CH11231.

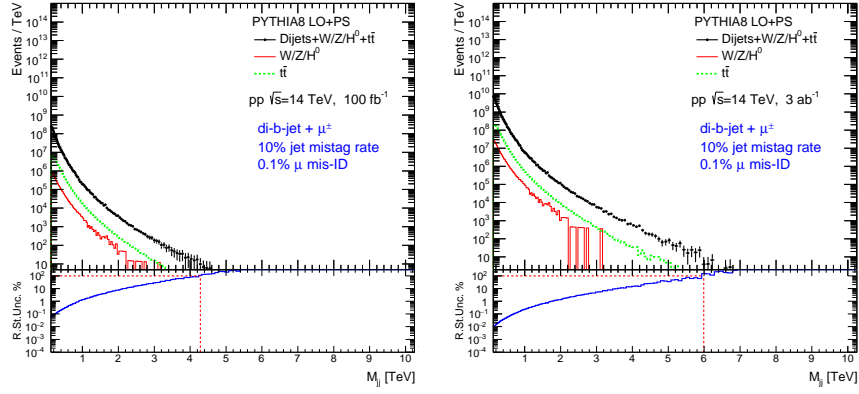
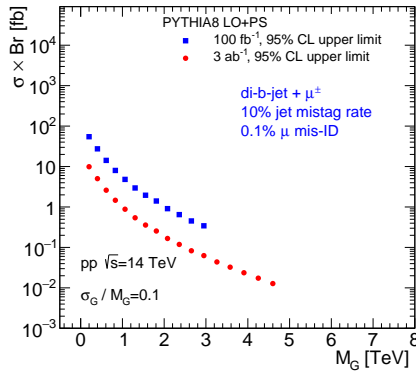
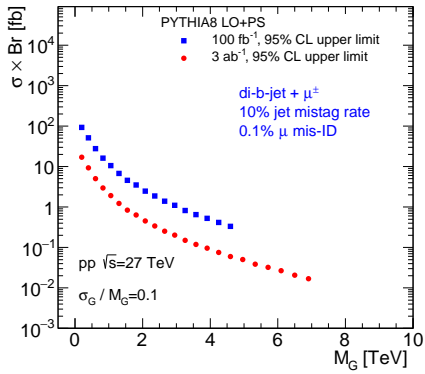
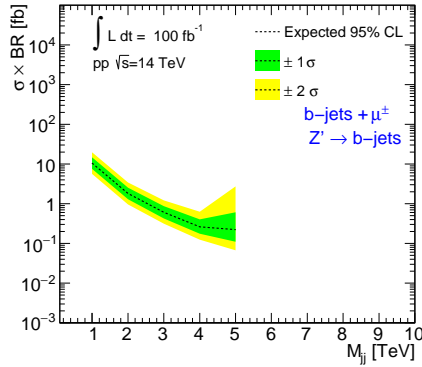
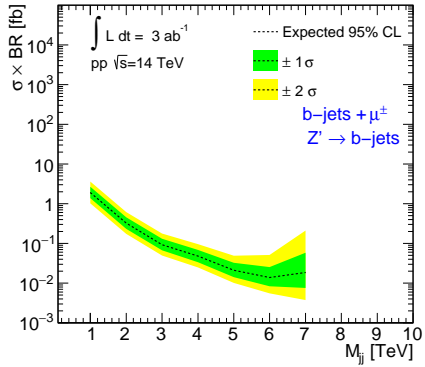
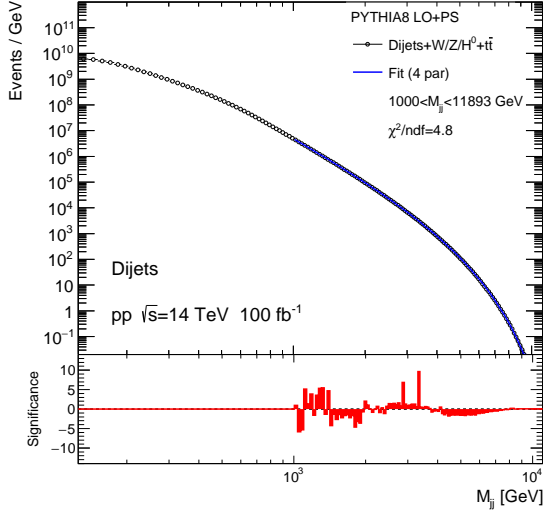
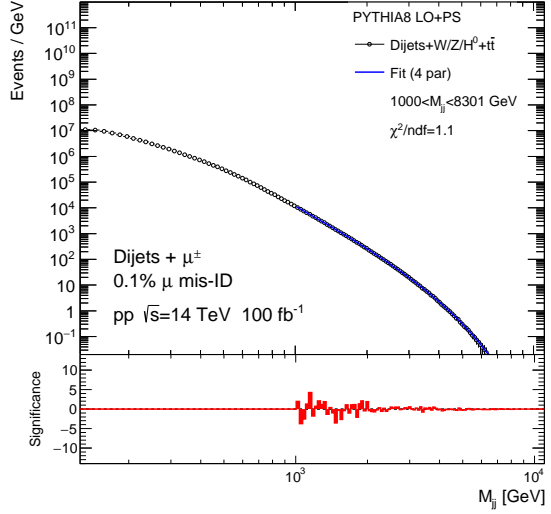
(a) 100 fb^{-1} (b) 3 ab^{-1} (c) 100 fb^{-1} (d) 3 ab^{-1} (e) 100 fb^{-1} (f) 3 ab^{-1}

FIG. 17. (a)-(b) show the distribution of dijet invariant masses with jets identified as b -jets, in events with associated muons for 100 fb^{-1} and 3 ab^{-1} . (c)-(d) 95% C.L. upper limits obtained from the on cross section times the branching ratio to two jets for a hypothetical signal approximated by a Gaussian contribution to the expected dijet mass. The limits are obtained for events with isolated muons. (e)-(f) 95% C.L. upper limits for a Z' particle decaying to two jets for the centre-of-mass energy of 14 TeV.

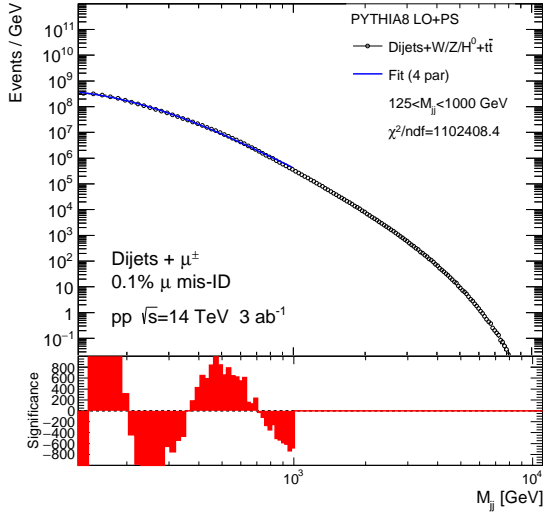


(a)Dijets at 14 TeV

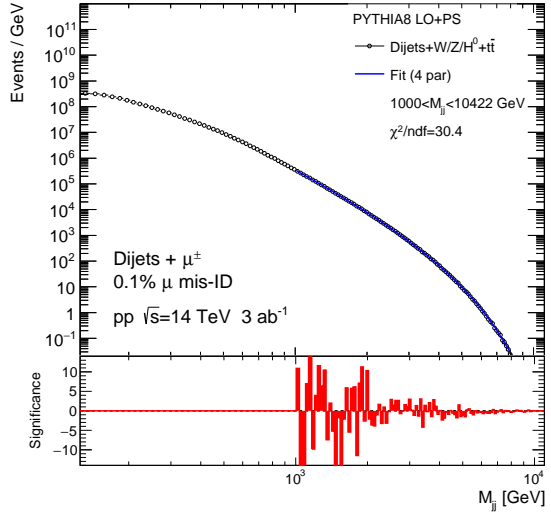


(b)Dijets plus muon at 14 TeV

FIG. 18. Dijet invariant masses shown together with the analytic fit function Eq. 1 after the χ^2 minimization. The simulations were performed for (a) inclusive dijet events and (b) for dijet events with associated muon. The results are obtained using 100 fb^{-1} .



(a)14 TeV, 3 ab^{-1} , $125 < M_{jj}^{fit} < 1 \text{ TeV}$



(b)14 TeV, 3 ab^{-1} , $M_{jj}^{fit} > 1 \text{ TeV}$

FIG. 19. Dijet invariant masses in events with muons with $p_T > 60 \text{ GeV}$ fitted with the analytic function Eq. 1 for different mass ranges. The simulations are shown for the HL-LHC collider.

REFERENCES

- [1] G. Aad *et al.* (ATLAS), *Phys. Lett.* **B754**, 214 (2016), [arXiv:1511.00502 \[hep-ex\]](#).
- [2] G. Aad *et al.* (ATLAS), *Physics Letters B* **759**, 229 (2016).
- [3] M. Aaboud *et al.* (ATLAS), *Phys. Rev.* **D96**, 052004 (2017), [arXiv:1703.09127 \[hep-ex\]](#).
- [4] V. Khachatryan *et al.* (CMS), *Phys. Rev. Lett.* **105**, 211801 (2010), [arXiv:1010.0203 \[hep-ex\]](#).
- [5] S. Chatrchyan *et al.* (CMS), *Phys. Rev.* **D87**, 114015 (2013), [arXiv:1302.4794 \[hep-ex\]](#).
- [6] A. M. Sirunyan *et al.* (CMS), *Phys. Lett.* **B769**, 520 (2017), [Erratum: *Phys. Lett.*B772,882(2017)], [arXiv:1611.03568 \[hep-ex\]](#).
- [7] M. Strassler, “Finding new physics hidden in the bulk of SM distributions,” (2016), Presentation at the Boost2016 workshop, Oxford.
- [8] M. J. Strassler and K. M. Zurek, *Phys. Lett.* **B651**, 374 (2007), [arXiv:hep-ph/0604261 \[hep-ph\]](#).
- [9] T. Sjostrand, S. Mrenna, and P. Z. Skands, *JHEP* **05**, 026 (2006), [arXiv:hep-ph/0603175](#); *Comput. Phys. Commun.* **178**, 852 (2008), [arXiv:0710.3820 \[hep-ph\]](#).
- [10] ATLAS Collaboration, *ATLAS Run 1 Pythia8 tunes*, Tech. Rep. ATL-PHYS-PUB-2014-021 (CERN, Geneva, 2014).
- [11] R. D. Ball *et al.*, *Nucl. Phys.* **B867**, 244 (2013), [arXiv:1207.1303 \[hep-ph\]](#); R. D. Ball *et al.* (NNPDF), *JHEP* **04**, 040 (2015), [arXiv:1410.8849 \[hep-ph\]](#).
- [12] A. Buckley, J. Ferrando, S. Lloyd, K. Nordström, B. Page, M. Rfenacht, M. Schnherr, and G. Watt, *Eur. Phys. J.* **C75**, 132 (2015), [arXiv:1412.7420 \[hep-ph\]](#).
- [13] M. L. Mangano, M. Moretti, F. Piccinini, R. Pittau, and A. D. Polosa, *JHEP* **0307**, 001 (2003), [arXiv:hep-ph/0206293 \[hep-ph\]](#).
- [14] Z. Bern, K. Ozeren, L. J. Dixon, S. Hoeche, F. Febres Cordero, *et al.*, *PoS* **LL2012**, 018 (2012), [arXiv:1210.6684 \[hep-ph\]](#).
- [15] S. V. Chekanov, *Adv. High Energy Phys.* **2015**, 136093 (2015), <http://atlaswww.hep.anl.gov/hepsim/>, [arXiv:1403.1886 \[hep-ph\]](#).
- [16] P. Langacker, *Rev. Mod. Phys.* **81**, 1199 (2009), [arXiv:0801.1345 \[hep-ph\]](#).
- [17] M. Cacciari, G. P. Salam, and G. Soyez, *JHEP* **04**, 063 (2008), [arXiv:0802.1189 \[hep-ph\]](#).

- [18] M. Cacciari, G. P. Salam, and G. Soyez, *Eur. Phys. J. C* **72**, 1896 (2012), <http://fastjet.fr/>, arXiv:1111.6097 [hep-ph].
- [19] G. Aad *et al.* (ATLAS), “Expected Performance of the ATLAS Experiment - Detector, Trigger and Physics,” CERN-OPEN-2008-020 (2009), arXiv:0901.0512 [hep-ex].
- [20] G. Aad *et al.* (ATLAS), *JINST* **11**, P04008 (2016), arXiv:1512.01094 [hep-ex].
- [21] G. Aad *et al.* (ATLAS), *Phys. Lett. B* **754**, 302 (2016), arXiv:1512.01530 [hep-ex].
- [22] M. Baak, G. J. Besjes, D. Cte, A. Koutsman, J. Lorenz, and D. Short, *Eur. Phys. J. C* **75**, 153 (2015), arXiv:1410.1280 [hep-ex].
- [23] G. Cowan, K. Cranmer, E. Gross, and O. Vitells, *Eur. Phys. J. C* **71**, 1554 (2011), [Erratum: *Eur. Phys. J. C* **73**, 2501 (2013)], arXiv:1007.1727 [physics.data-an].
- [24] Data analyses that use a complex trigger menu with a mixture of prescaled and unprescaled triggers are possible, but such studies require a significant effort and, as the result, are rather rare.
- [25] F. Huang, C. Osman, and T. R. Ophel, *Nucl. Instr. and Methods* **68**, 141 (1969); M. Mariscotti, *Nucl. Instr. and Methods* **50**, 309 (1967); K. J. Blinowska and E. F. Wessner, *Nucl. Instr. and Methods* **118**, 597 (1974); Z. K. Silagadze, *Nucl. Instrum. and Methods* **A376**, 451 (1996), arXiv:hep-ex/9506013 [hep-ex]; M. Morháč, J. Kliman, V. Matoušek, M. Veselský, and I. Turzo, *Nucl. Instr. and Methods in Physics Research A* **443**, 108 (2000); S. V. Chekanov and M. Erickson, *Adv. High Energy Phys.* **2013**, 162986 (2013), arXiv:1110.3772 [physics.data-an]; M. Frate, K. Cranmer, S. Kalia, A. Vandenberg-Rodes, and D. Whiteson, (2017), arXiv:1709.05681 [physics.data-an].